

Green-Kubo relation for viscosity tested using experimental data for a two-dimensional dusty plasma

Yan Feng,^{*} J. Goree, and Bin Liu*Department of Physics and Astronomy, The University of Iowa, Iowa City, Iowa 52242, USA*

E. G. D. Cohen

*The Rockefeller University, 1230 York Avenue, New York, New York 10065, USA and**Department of Physics and Astronomy, The University of Iowa, Iowa City, Iowa 52242, USA*

(Received 1 July 2011; revised manuscript received 16 September 2011; published 28 October 2011)

The theoretical Green-Kubo relation for viscosity is tested using experimentally obtained data. In a dusty plasma experiment, micron-sized dust particles are introduced into a partially ionized argon plasma, where they become negatively charged. They are electrically levitated to form a single-layer Wigner crystal, which is subsequently melted using laser heating. In the liquid phase, these dust particles experience interparticle electric repulsion, laser heating, and friction from the ambient neutral argon gas, and they can be considered to be in a nonequilibrium steady state. Direct measurements of the positions and velocities of individual dust particles are then used to obtain a time series for an off-diagonal element of the stress tensor and its time autocorrelation function. This calculation also requires the interparticle potential, which was not measured experimentally but was obtained using a Debye-Hückel-type model with experimentally determined parameters. Integrating the autocorrelation function over time yields the viscosity for shearing motion among dust particles. The viscosity so obtained is found to agree with results from a previous experiment using a hydrodynamical Navier-Stokes equation. This comparison serves as a test of the Green-Kubo relation for viscosity. Our result is also compared to the predictions of several simulations.

DOI: [10.1103/PhysRevE.84.046412](https://doi.org/10.1103/PhysRevE.84.046412)

PACS number(s): 52.27.Lw, 52.27.Gr, 66.20.-d, 83.85.Jn

I. INTRODUCTION

There are various two-dimensional (2D) physical systems that allow for direct observation of individual particle dynamics. These systems include colloidal suspensions [1], granular materials [2], electrons on a liquid helium surface in a Wigner lattice [3], ions confined magnetically in a Penning trap [4], and single-layer dusty plasmas [5–8]. In these systems, the relevant particles collide with their neighbors frequently, so that momentum and energy are transported from one place to another. (In all these 2D physical systems, motion is not purely 2D, but usually includes some limited out-of-plane motion, so that the systems are often described as quasi-2D.)

Shear viscosity, η , is a transport coefficient that characterizes the momentum flux perpendicular to a velocity gradient. Sustaining the velocity gradient requires the application of a shear stress, which corresponds to an off-diagonal element of a stress tensor. The hydrodynamical definition of shear viscosity is the ratio of this off-diagonal element and the velocity gradient [9]. As a measure of dissipation, viscosity is useful, for example, in describing the damping of shear waves [10–12].

The Green-Kubo relation for viscosity, as described in Sec. II, enables a calculation of viscosity using as its input a time-series record of the motion of individual particles [13–15]. The relation is based on fluctuations, not a macroscopic velocity gradient. Until now, the Green-Kubo relation for viscosity has been widely used with an input of data from molecular dynamics (MD) *simulations* (see, for example, [16]), but not with data from *experiments*.

Viscosity is most commonly determined in experiments using a macroscopic velocity gradient. For example, in a rheometer [17], a stress is applied by a moving boundary, causing the liquid to flow with a velocity gradient, so that the viscosity can be determined using its hydrodynamical definition. Another experimental approach, which is used with experimental data from colloidal suspensions and other soft materials without macroscopic velocity gradients, is the measurement of the mean-square displacement (MSD) of individual particles and the assumption that the Stokes-Einstein relation is valid, allowing then a calculation of viscosity from the measured MSD [18,19], as discussed in Sec. II. All of these experimental methods are different from the use of the Green-Kubo relation.

It has been questioned whether transport coefficients exist in 2D systems. Molecular dynamics simulations suggested that the diffusion, viscosity, and thermal conductivity coefficients would not exist in a 2D system of *hard disks* [20]. This result led to theoretical investigations that indicated the time integral in the Green-Kubo relations diverges and the corresponding transport coefficients in 2D systems are nonexistent [21]. We will discuss this issue of convergence in Sec. IV E.

In this paper, we test the Green-Kubo relation with an input of experimental data from a quasi-2D dusty plasma. The dust particles in a dusty plasma, unlike hard disks, have a relatively long-range interparticle interaction.

Our results and conclusions in this paper are intended to have a usefulness that extends beyond the area of dusty plasmas. Accordingly, we have attempted to make our presentation accessible to scientists who are not specialists in that area. The experimental data used in this paper are from an experiment by Feng *et al.* [8]. We will introduce the concepts of dusty

^{*}yan-feng@uiowa.edu

plasmas, along with some key aspects of the experiment, below as well as in Sec. III. Further details of the experiment can be found in [8].

A dusty plasma is a *four-component* mixture consisting of micron-size particles of solid matter, a gas of neutral atoms, free electrons, and free positive ions. We will refer in this paper to the particles of solid matter as “dust particles.” In experiments, the gas is often argon, and so are the ions. The electrons and positive ions are present because of electric fields, provided by a power supply, which lead to a weak ionization of the neutral argon gas. Because of the much larger mobility of the electrons, as compared to the ions, many more electrons are collected on the dust particles, so that a dust particle develops a large negative electric charge, comparable to thousands of elementary charges [22]. The electrons and ions that surround a negatively charged dust particle are rearranged, resulting in a screening layer with a surplus of positive ions that surrounds the dust particle. Because of the complicated interactions among its four components, a dusty plasma is sometimes termed a “complex plasma” [23]. While the gas, electrons, and ions fill a 3D vacuum chamber, the dust particles do not. They are levitated against the downward force of gravity by a strong vertical electric field. In the experiment [8], enough dust particles were introduced to fill a single horizontal layer, but not enough to begin filling a second layer. The dust particles were not in contact with any solid boundary, but they suffer a friction due to the surrounding neutral argon gas. In this paper, we will always consider the gas atoms as a whole to be a continuum, but we will consider the dust particles as individual entities.

The experiment [8] can be described as quasi-2D. The dust particles, although they are three-dimensional, are arranged in two dimensions. It was verified, using video observations, that the dust particle motion in the vertical direction was extremely limited, as compared to that in the horizontal direction, so that dust particles moved past one another only as a result of their horizontal motion.

The neutral argon gas is rarefied in the experiment [8]. At a density five orders of magnitude less than in a standard atmosphere, collisions among gas atoms have a long mean free path, on the order of 1 cm. The effect of these collisions on the dust particles is much diminished because the dust particles occupy only a thin 2D layer, so that a gas atom that collides with a dust particle is likely to be knocked out of the layer of the dust particles [24]. Thus, no significant transfer of momentum between two dust particles can occur due to the first one colliding with a gas atom that then collides with the second dust particle. The only interaction between dust particles and gas that we must consider is the frictional drag force F_f on the dust particle, which is proportional to the relative velocity between the dust particle and the gas as a whole. In [8], the gas flow was negligibly slow.

Since it is only the motion of the dust particles that will be of interest here, we will simplify our description of the four-component mixture. The dust particles are assumed to interact among themselves with a screened Coulomb repulsion, as discussed in Sec. IV. The role of the electrons and ions is then only to modify the interparticle potential and provide the screening. Thus, in our simplified description of the four-component mixture, we consider only a *binary mixture*: first,

moving charged dust particles whose interaction potential is a screened Coulomb repulsion, and second, a stationary neutral gas that exerts a frictional drag on moving dust particles.

This reduction of a four-component mixture to a binary mixture, in which all the properties of the electrons and ions are contained in the screening, has been used previously in theoretical descriptions of dusty plasmas, for example in the analysis of wave propagation [25]. When using this binary-mixture description, one could consider a charged dust particle as a “dressed particle” [26] consisting of a micron-sized solid core that is negatively charged and a larger surrounding screening region that is positively charged. The center of this dressed particle corresponds to what is observed experimentally by video microscopy.

In the experiment [8], the repulsion between dust particles was so strong that the dust particles self-organized in a solidlike arrangement called a Wigner crystal [27]. In order to study a liquid and its viscosity, this solid was melted by increasing the kinetic energy of the dust particles, which was done by using the laser-heating method [28].

When we refer in this paper to viscosity, it is only the motion of the dust particles that we directly take into account. In our simplified description of a dusty plasma, treating it as a binary mixture of dust particles and gas, we do not consider the momentum carried by electrons and ions. Moreover, a transfer of momentum between two dust particles does not occur due to the first dust particle colliding with a gas atom that then collides with the second, as discussed above. Thus, in our simplified binary-mixture description, the viscosity describes motion of only dust particles [29].

Previously, viscosity was studied in other dusty plasma experiments by applying a macroscopic shear stress using laser manipulation [30–33] to generate a macroscopic velocity gradient, and using a hydrodynamical approach to calculate the viscosity based on the measured velocity profile of the dust particles. In the test reported in this paper, we will compare the hydrodynamical result of [31] to the viscosity determined using a theoretical Green-Kubo relation with an input of data from the experiment of [8], which was performed without a macroscopic velocity gradient.

In Sec. II, the Green-Kubo relation for viscosity is reviewed. In Sec. III, we provide further details of the experiment [8]. In Sec. IV, we introduce how we use the Green-Kubo relation with an input of experimental data. In Sec. V, we report our MD simulations of the experiment [8]. We determine the viscosity in Sec. VI, and in Sec. VII this result using the Green-Kubo relation is compared to the results of a previous experiment using a hydrodynamical method [31]. In Sec. VII, we also provide a comparison to the results of previous computer simulations [24,34,35].

II. GREEN-KUBO RELATION

To obtain transport coefficients such as diffusion, viscosity, and thermal conductivity in a liquid, Green-Kubo relations [13–15,34,36] are often used. Their required inputs include time series for the positions and velocities of particles. The simplest of these Green-Kubo relations is the one for diffusion. It can be derived easily using the physical assumption that the MSD for fluctuating particle displacements is proportional to

the diffusion coefficient and the time [15]. The derivation of the Green-Kubo relation for viscosity is less trivial, and it is based on the fluctuating stress, not an MSD [37]. Here we review the standard Green-Kubo relation for calculating viscosity, in three steps, as it is used for all kinds of liquids, not just dusty plasmas in a liquid phase.

In the first step, an off-diagonal element of the stress tensor $P_{xy}(t)$ is defined by

$$P_{xy}(t) = \sum_{i=1}^N \left[m v_{ix} v_{iy} - \frac{1}{2} \sum_{j \neq i}^N \frac{x_{ij} y_{ij}}{r_{ij}} \frac{\partial \Phi(r_{ij})}{\partial r_{ij}} \right], \quad (1)$$

where i and j denote different particles, N is the total number of particles of mass m , $\mathbf{r}_i = (x_i, y_i)$ is the position of particle i , $x_{ij} = x_i - x_j$, $y_{ij} = y_i - y_j$, $r_{ij} = |\mathbf{r}_i - \mathbf{r}_j|$, and $\Phi(r_{ij})$ is the interparticle potential energy. Although not indicated in Eq. (1), the positions and velocities of particles vary with time, and this accounts for the time dependence of $P_{xy}(t)$. In the second step, an autocorrelation function of $P_{xy}(t)$ is calculated as

$$C_\eta(t) = \langle P_{xy}(t) P_{xy}(0) \rangle. \quad (2)$$

We will refer to $C_\eta(t)$ as the stress autocorrelation function (SACF). The brackets $\langle \cdot \cdot \cdot \rangle$ denote an average over an equilibrium ensemble, which in practice is often replaced by an average over different initial conditions. In the third step, the SACF is integrated over time to yield the viscosity η ; for a 2D system, the result is

$$\eta = \frac{1}{Ak_B T} \int_0^\infty C_\eta(t) dt, \quad (3)$$

where A is the area of the 2D system and T is its temperature. Equation (3) combined with Eq. (2) represent the Green-Kubo relation for viscosity in 2D. Similar Green-Kubo relations can be written for diffusion, thermal conductivity, and bulk viscosity [15,36].

Viscosity η and mass density ρ have different dimensions in 2D and 3D. The units of η are kg s^{-1} in 2D and $\text{kg m}^{-1} \text{s}^{-1}$ in 3D. Correspondingly, in the denominator of Eq. (3) we have replaced the usual volume for a 3D system with an area A for the 2D system. In 2D, the areal mass density is $\rho = nm$ with units of kg m^{-2} , where n is the areal number density. We will report results for the kinematic viscosity η/ρ , which has the same units in 2D and 3D.

While Green-Kubo relations have been commonly used in computer simulations to obtain transport coefficients, their use with experimental data is uncommon. We are aware of only one previous calculation of any transport coefficient using the input of experimental data in a Green-Kubo relation. Using an input of data consisting of time series of velocities of particles determined from time series of measured particle positions in a dusty plasma experiment, Vaulina *et al.* [38,39] obtained the diffusion coefficient, D . In their pioneering work, they obtained D using the Green-Kubo relation for diffusion, which is a time integration of the velocity autocorrelation function.

In principle, the approach of Vaulina *et al.* of using a Green-Kubo relation to obtain the diffusion coefficient could be extended to other transport coefficients, namely the viscosity, thermal conductivity, and bulk viscosity. Such an extension is nontrivial because these Green-Kubo relations

require time-series data not only for particle velocities but also for interparticle potential. This potential generally cannot be measured directly in dusty plasma experiments such as [8,38,39]. In extending the approach of Vaulina *et al.* [38,39] to viscosity, we overcome the lack of an experimentally measured potential by calculating the potential using a theoretical model. This is done using experimentally determined parameters for the model together with measured particle positions, as described in Sec. IV A.

Besides using the Green-Kubo relation, another way to obtain the viscosity of fluids without a macroscopic velocity gradient is the use of microrheology methods [18,19]. In this approach, the MSD of individual microparticles is measured, and the Stokes-Einstein relation is assumed to be valid [18,19]. The Stokes-Einstein relation [40] is a combination of the Stokes law, which is a hydrodynamic treatment for viscous flow at a low Reynolds number, and the Einstein relation, which relates a diffusion coefficient for Brownian motion and a frictional force. This MSD-based method has been used in physical systems like colloidal suspensions, where a microparticle's motion is overdamped due to the surrounding liquid solvent [18,19].

The Green-Kubo relation for viscosity is different from MSD-based approaches of determining viscosity. The derivation of the Green-Kubo relation centers on the fluctuations of the stress P_{xy} , and it does not rely on the validity of a diffusion coefficient. There is evidence that the Stokes-Einstein relation is not valid for 2D dusty plasmas [41]. Moreover, it is possible that a physical system can have a valid viscosity coefficient but lack a valid diffusion coefficient, for example due to superdiffusion, as has been suggested for 2D systems such as Yukawa liquids [36].

III. EXPERIMENTAL INPUT

Before reviewing the experiment [8], we will discuss a few properties of dusty plasmas and their relevant length and time scales.

When dust particles have a charge of several thousand elementary charges, their interparticle potential energy Φ can be larger than their kinetic energy. In this case, the collection of dust particles is said to be a ‘‘strongly coupled plasma’’ [42,43]. A measure of strong coupling is the Coulomb coupling parameter $\Gamma \equiv (Q^2/4\pi\epsilon_0 a k_B T)$, where Q is the charge of the dust particle, ϵ_0 is the permittivity of free space, a is a typical interparticle distance as defined below, and T is the kinetic temperature of the dust particles. The Coulomb coupling parameter is essentially a ratio of interparticle potential energy and kinetic energy. A plasma is strongly coupled when $\Gamma > 1$, and it can behave like a liquid or a Wigner crystal. In a dusty plasma, the dust particles are usually strongly coupled due to their large charge Q . The electrons and the ions have a much smaller charge, and in most plasmas they are not strongly coupled, unless great efforts are made to cool them to low temperatures [4].

The length scales of a dusty plasma include the screening length λ_D and the typical distance between dust particles. In the dusty plasma literature, the typical distance between dust particles is commonly reported either as the lattice constant b for a Wigner crystal or as $a = (n\pi)^{-1/2}$ for a liquid, where

n is the areal number density. In the literature for strongly coupled plasmas, a is called the 2D Wigner-Seitz radius [42]. All three of these length scales, λ_D , b , and a , are typically on the order of 1 mm. The diameter of a dust particle is typically a few microns, which is much smaller than any of these length scales, and also much smaller than the mean free path for collisions among the rarefied argon gas atoms.

The *time scales* of a dusty plasma include measures of collective motion among the dust particles and of the frictional drag experienced by a dust particle due to the gas as a whole. The former is quantified by the 2D plasma frequency for dust particles, $\omega_{pd} = (Q^2/2\pi\epsilon_0 m a^3)^{1/2}$ [42], where the subscripts p and d refer to plasma and dust, respectively. The frictional drag experienced by a dust particle due to the neutral argon gas is quantified by a friction coefficient, which is commonly defined in the literature for dusty plasmas as $\nu_f = F_f/mv$, where F_f is the gas friction force experienced by one dust particle and mv is the momentum of the same particle. This coefficient has the dimension of inverse time, and a typical value for a micron-sized dust particle in a rarefied gas is $\nu_f \approx 1 \text{ s}^{-1}$. If the gas is sufficiently rarefied, $\omega_{pd} > \nu_f$, so that the dust particle motion is said to be underdamped.

We now summarize some aspects of the experiment [8] that are relevant for our analysis. The dust particles were polymer microspheres of $8.1 \mu\text{m}$ diameter. They were levitated by a vertical dc electric field to form a single horizontal layer, as sketched in Fig. 1. Radial dc electric fields provided horizontal confinement so that the dust particles filled a circular region of diameter 52 mm.

For each experimental run, one movie of dust particle motion was recorded. A Phantom v5.2 high-speed camera viewed the dust particles from above. It was operated at 250 frames/s, so that data were recorded with a time interval $\Delta t = 4 \text{ ms}$. The duration of a movie, 20 s, was limited by the camera’s memory. The camera’s field-of-view (FOV) included $N \approx 2100$ dust particles. Two of the required inputs for Eq. (1), the positions and velocities of the dust particles, were obtained using the moment method [44] and particle tracking [45]. The interparticle distance, averaged over the camera’s FOV, was characterized by $b = 0.67 \text{ mm}$ in the Wigner crystal and $a = 0.35 \text{ mm}$ in the liquid.

A total of seven runs were performed. Three runs without laser heating were made to determine the interparticle potential energy in the Wigner crystal. Four runs were done with laser heating to make the liquid, and they provide the data that we will use here as the input for the Green-Kubo relation to determine viscosity in the liquid phase.

The laser heating method [46] uses the radiation pressure due to laser beams, which are directed toward the dust particles by scanning mirrors [47], which we configured as in [28,48]. Laser heating increases the kinetic temperature of dust particles without changing their charge. The velocity distribution function has been observed to be nearly Maxwellian [28]. In the experiment [8], the kinetic temperature T , calculated from the mean-square velocity [49], was $2.5 \times 10^4 \text{ K}$ in the liquid (with laser heating), and 10^3 K in the Wigner crystal (without laser heating). The temperature was nearly uniform spatially, which is desirable because viscosity varies with temperature.

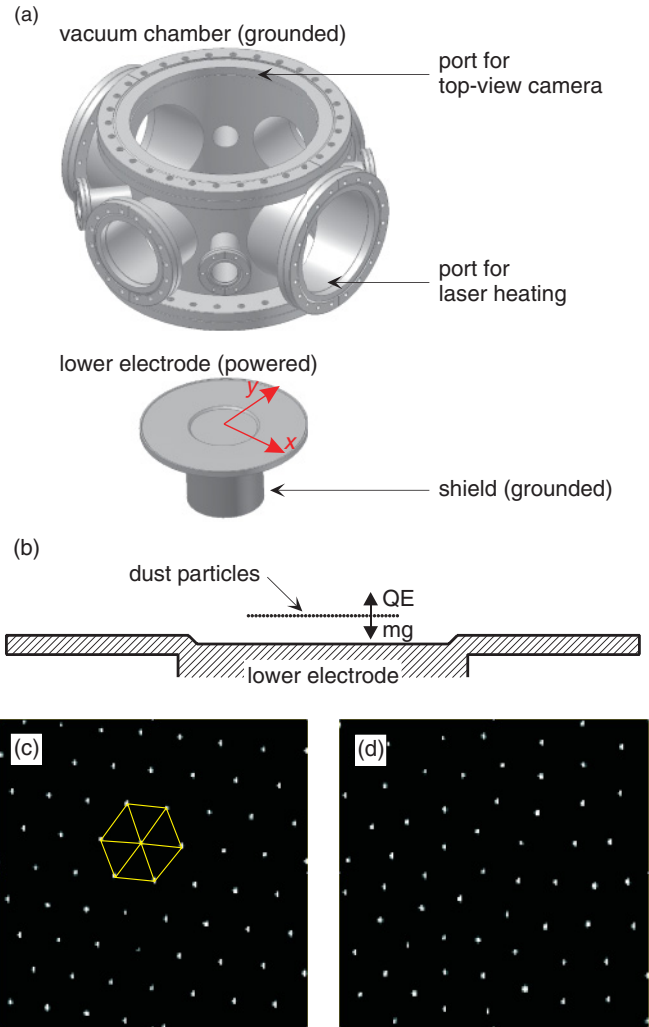


FIG. 1. (Color online) Configuration for the experiment [8]. (a) This diagram of the vacuum chamber is shown in an exploded view to better show the lower electrode, which in the experiment was located inside the chamber. A low-pressure gas of neutral argon atoms filled the chamber. A radiofrequency voltage was applied between two electrodes, separated by an insulator. One electrode was the powered lower electrode, and the other consisted of the grounded vacuum chamber and shield. The gas was partially ionized, yielding a plasma with three components: electrons, positive argon ions, and neutral argon atoms. The x and y axes correspond to the two orthogonal directions used in measuring the positions and velocities of dust particles. The side ports were used to admit laser beams, not shown here. For heating, a pair of 532 nm laser beams were directed into the chamber by scanning mirrors as in [28], while for illumination a 577 nm laser sheet was used with a configuration as in [47]. (b) This sketch shows a side view of the lower electrode. Polymer microspheres were introduced by shaking them into the plasma from above, and they moved downward due to gravity g . They gained a negative electric charge Q and were levitated upward due to a vertical dc electric field E so that they remained in a single horizontal layer above the lower electrode. There was also a smaller radial dc electric field, not shown, which provided horizontal confinement. Images of the dust particles were recorded by a video camera viewing through the top port. Shown here are $5 \text{ mm} \times 5 \text{ mm}$ portions of two images: (c) a Wigner lattice without laser heating (lines have been drawn to indicate the lattice structure) and (d) a liquid maintained by laser heating.

IV. USING THE GREEN-KUBO RELATION WITH EXPERIMENTAL INPUT DATA

Calculations of viscosity with the Green-Kubo relation, Eqs. (1)–(3), must be adapted to use the experimental data as input, due to four difficulties. First, the experiment [8] provided direct measurements of x_i , y_i , v_{ix} , and v_{iy} , but not of the interparticle potential energy $\Phi(r_{ij})$. Second, the camera has a finite FOV, so that we do not have data for all dust particles in the 2D layer. Third, the motion of dust particles may include a local macroscopic flow, i.e., a nonzero time-average velocity. Fourth, the data for the positions and velocities of the dust particles are recorded as a time series of a finite duration, so that the integral in Eq. (3) must have a finite limit. We will take all this into account by making a number of approximations in the Green-Kubo calculations. We will next describe these approximations as well as discuss the validity of the results that are obtained.

A. Interparticle potential

To solve the first difficulty, a lack of experimental measurements of the interparticle potential energy $\Phi(r_{ij})$, we will use a model for these energies when calculating the off-diagonal element of the stress tensor P_{xy} . For a single-layer dusty plasma like ours, models that have been tested successfully include an isotropic repulsion according to the 3D Debye-Hückel potential [50],

$$\phi(r_{ij}) = \frac{Q}{4\pi\epsilon_0} \frac{\exp(-r_{ij}/\lambda_D)}{r_{ij}}, \quad (4)$$

as well as more complicated isotropic [51] and nonisotropic interactions [52]. Here we will use the Debye-Hückel potential, Eq. (4), where i and j are dust particles of charge Q separated by a distance r_{ij} , and λ_D is the screening length due to electrons and ions. The corresponding potential energy is $\Phi(r_{ij}) = Q\phi(r_{ij})$. In the literature for dusty plasmas, it is common to name Eq. (4) after Yukawa rather than Debye and Hückel. This potential has been used in theoretical and simulation studies of viscosity in strongly coupled plasmas; see, for example [36,53–56].

Two parameters in Eq. (4), Q and λ_D , were determined in the experiment [8] using a phonon-spectra method [57,58] in the Wigner crystal. For the three experimental runs without laser heating, position and velocity measurements were used to compute the phonon spectra, which were compared to theoretical wave dispersion relations [25] that assume Eq. (4), yielding $\lambda_D = 0.70 \pm 0.14$ mm and $Q/e = -6000 \pm 600$, where e is the elementary charge. Using these two values along with measured particle positions and velocities, we can calculate P_{xy} and then the SACF [59].

Having determined Q and λ_D , we can calculate the values of other parameters. We find that the Coulomb coupling parameter is $\Gamma = 68$ for the liquid of dust particles. The dimensionless particle spacing [42] is $\kappa \equiv a/\lambda_D = 0.5 \pm 0.1$. We also calculated $\omega_{pd} = 30 \pm 3$ s⁻¹. We note that ω_{pd} is significantly larger than the gas friction coefficient $\nu_f = 2.4$ s⁻¹, indicating that dust particle motion is underdamped.

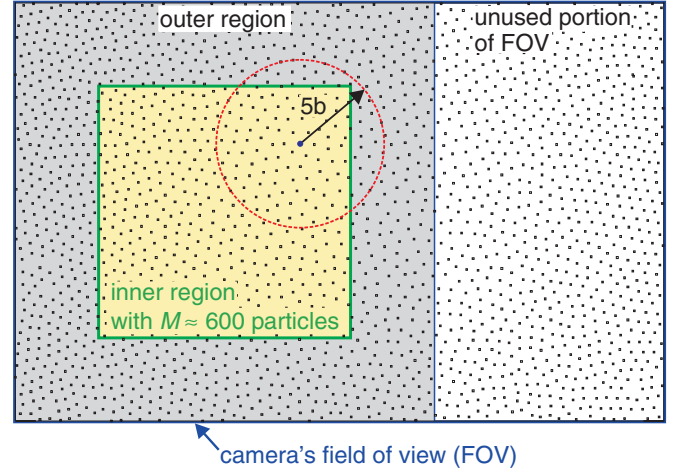


FIG. 2. (Color online) Sketch of the division of the camera FOV into inner and outer regions for the experiment [8]. In Eq. (5), the subscripts i and j refer to particles located in the inner region and both the inner and outer regions, respectively. The circle indicates the cutoff distance $5b$ for the potential. The unused portion of the camera FOV on the right is not included in the analysis.

B. Finite field of view

To solve our second difficulty, the finite FOV of the camera that limits us to recording data for only a portion of the dust particles, we will *cut off* the interparticle potential in Eq. (4) at large distances. In addition, we will *divide* the FOV into inner and outer regions, Fig. 2. The cutoff is done at a large interparticle distance of $5b$, where the exponential in Eq. (4) is $< 10^{-2}$.

The FOV is divided into inner and outer regions because the potential energy of a dust particle cannot be obtained meaningfully if it is located near the edge of the FOV, due to interactions with dust particles of unknown positions outside the FOV. Therefore, dust particles in the outer region are used only to calculate the potential energies Φ of dust particles in the inner region. In other words, when calculating P_{xy} , we limit the dust particles i to those that are located within the inner region, and we account for their interaction with other dust particles j located in *both* the inner and outer regions, as shown in Fig. 2. The outer region has a width of $5b$ to allow for a cutoff radius of $5b$, and the inner region is $22.0b \times 23.7b$ (i.e., 14.8×15.9 mm²). Because of this different treatment of dust particles in the inner and outer regions, we calculate P_{xy} as

$$P_{xy} = \sum_{i=1}^M \left[m v_{ix} v_{iy} - \frac{1}{2} \sum_{j \neq i}^N \frac{x_{ij} y_{ij}}{r_{ij}} \frac{\partial \Phi(r_{ij})}{\partial r_{ij}} \right], \quad (5)$$

where the stress P_{xy} is (implicitly) a function of time. All time series data are recorded at a time interval $\Delta t = 4$ ms. For the experiment [8], $M \approx 600$ dust particles are in the inner region while $N \approx 2100$ are in both regions combined. Both N and M fluctuate slightly with time, as dust particles move across the edges of the regions, but not enough to affect the result for viscosity significantly.

C. Nonzero time averages

Our third difficulty to solve is that the average velocity inside the FOV is not zero, due to finite macroscopic flow velocities of the dust particles, despite efforts that were made in the experiment [8] to avoid them. When computing the stress, the dust particle velocities are assumed to fluctuate about an average value of zero. In fact, a nonzero average velocity would contribute an unwanted constant value to the P_{xy} time series when computed using Eq. (1) or (5), which would cause the SACF, C_η , to decay to a nonzero value and introduce an unphysical contribution to the calculated viscosity. To solve this difficulty, without any approximation, we subtract from $P_{xy}(t)$ its time-average value, yielding then the fluctuating portion $\tilde{P}_{xy}(t)$. We then replace Eq. (2) for the SACF by

$$C_\eta(t) = \langle \tilde{P}_{xy}(t + t_0) \tilde{P}_{xy}(t_0) \rangle_0. \quad (6)$$

Here, the brackets $\langle \cdot \cdot \rangle_0$ in Eq. (6) denote an average over various initial times t_0 if the data are from a single run.

Our results for the SACF, for the four runs with laser heating, are shown in Fig. 3. All four runs show the same general trends, which resemble those seen in MD simulations as in [34].

D. Integration limit

To solve the fourth difficulty, the finite time duration of data, the viscosity η is computed with a finite upper limit in the time integral of the SACF. In principle, the upper limit should be infinite, as in Eq. (3), but we use

$$\eta = \frac{1}{Ak_B T} \int_0^{t'} C_\eta(t) dt, \quad (7)$$

and we follow the practice used in MD simulations of choosing the integration limit t' as the time when $C_\eta(t)$ crosses zero [60], as shown in Fig. 3. Because our time series $C_\eta(t)$ is noisy, we count a zero crossing only if it results in $C_\eta(t)$ remaining negative for at least $2\Delta t$. In Eq. (7), A is the area of the inner region.

E. Validity

For using the Green-Kubo relation to calculate viscosity with experimental input data, we should ask whether the approach is valid when it is used for a dusty plasma. We will mention three questions.

First, we note that the Green-Kubo relations are, strictly speaking, for the thermodynamic limit, where the number of dust particles and the system size tend to infinity while keeping the number density constant. In fact, the experiment has only thousands of dust particles. However, we believe that our experimental system size is large enough to use a Green-Kubo relation, as indicated by our system-size tests in Sec. V.

Second, we must consider the distinction between equilibrium and nonequilibrium systems. While our laser-heated dusty plasma is in a steady state, it is not in equilibrium. The collection of dust particles is best described as a driven-dissipative system [48], where the driving is mainly provided by the laser beams, and the dissipation is provided by gas-dust collisions as well as the dust-particle viscosity. Despite these

nonequilibrium conditions, however, the velocity distribution function for the dust particles has been observed to be nearly Maxwellian [28], as mentioned above. Thus, the statistics are close to those of an equilibrium system, which motivates us to use the Green-Kubo relation.

Third, we must ask whether long-time tails in the correlation function prevent the convergence of its integral, as was predicted theoretically [21] for 2D systems with hard-disk interparticle interactions. More recently, for a 2D system with a Debye-Hückel potential, simulations by Donkó *et al.* [36] indicated that long-time tails occur in some but not all cases. In particular, they reported that the SACF decays fast enough that its time integral η converges for a liquid at temperatures near the melting point, but not at absolute temperatures far above the melting point.

V. SIMULATIONS

To assess three sources of error mentioned in Sec. IV, viz., the potential cutoff, the FOV division, and the finite system size, we used MD simulations based on the Langevin equation [61]. In these simulations, we numerically integrate the Langevin equation to obtain the motion of each dust particle. This equation gives the force acting on a dust particle as a sum of three terms: an electric force due to all other dust particles using Eq. (4), a mean friction F_f due to the gas as a whole, as well as Gaussian random forces around this mean, to model the collisions of the dust particle with the neutral gas atoms [62,63].

Dust particle positions, velocities, and interaction energies were recorded at each time step of $0.019\omega_{pd}^{-1}$. We used $N = 4096$ particles in a 2D rectangular box with periodic boundary conditions. In a 2D Langevin MD simulation with a Debye-Hückel potential like ours, the equations of motion have three dimensionless parameters: the friction coefficient ν_f/ω_{pd} , the Coulomb coupling parameter Γ , and the dimensionless particle spacing κ . To mimic the experiment [8], we used $\nu_f/\omega_{pd} = 0.08$, $\Gamma = 68$, and $\kappa = 0.5$.

To test the effect of the cutoff, we carried out simulations at two cutoff distances to estimate the systematic error introduced in the last term of Eq. (5). In fact, we found that for a cutoff of $5b$, which we use in this paper, the viscosity result η was reduced by less than 5%, as compared to the result for a much larger cutoff of $13b$.

To test for errors arising from the division of the FOV, we compared results with and without the division, using Eqs. (5) and (1), respectively. We found the viscosity differed only negligibly.

Finally, to test for the effects of finite system size, we compared our Langevin MD simulation results for two sizes. Results for the larger system size of 4096 particles are reported in [24]. For the smaller size, to mimic the experiment [8], we used 48 simulation runs with $M = 600$ particles, as in the inner region for the experiment [8], for a duration [64] of $607\omega_{pd}^{-1}$. Comparing these two results for η , we find no statistically significant system-size effects. This test, shown in Table I, gives us confidence that the number of dust particles in [8] was not so small as to preclude using the Green-Kubo relation.

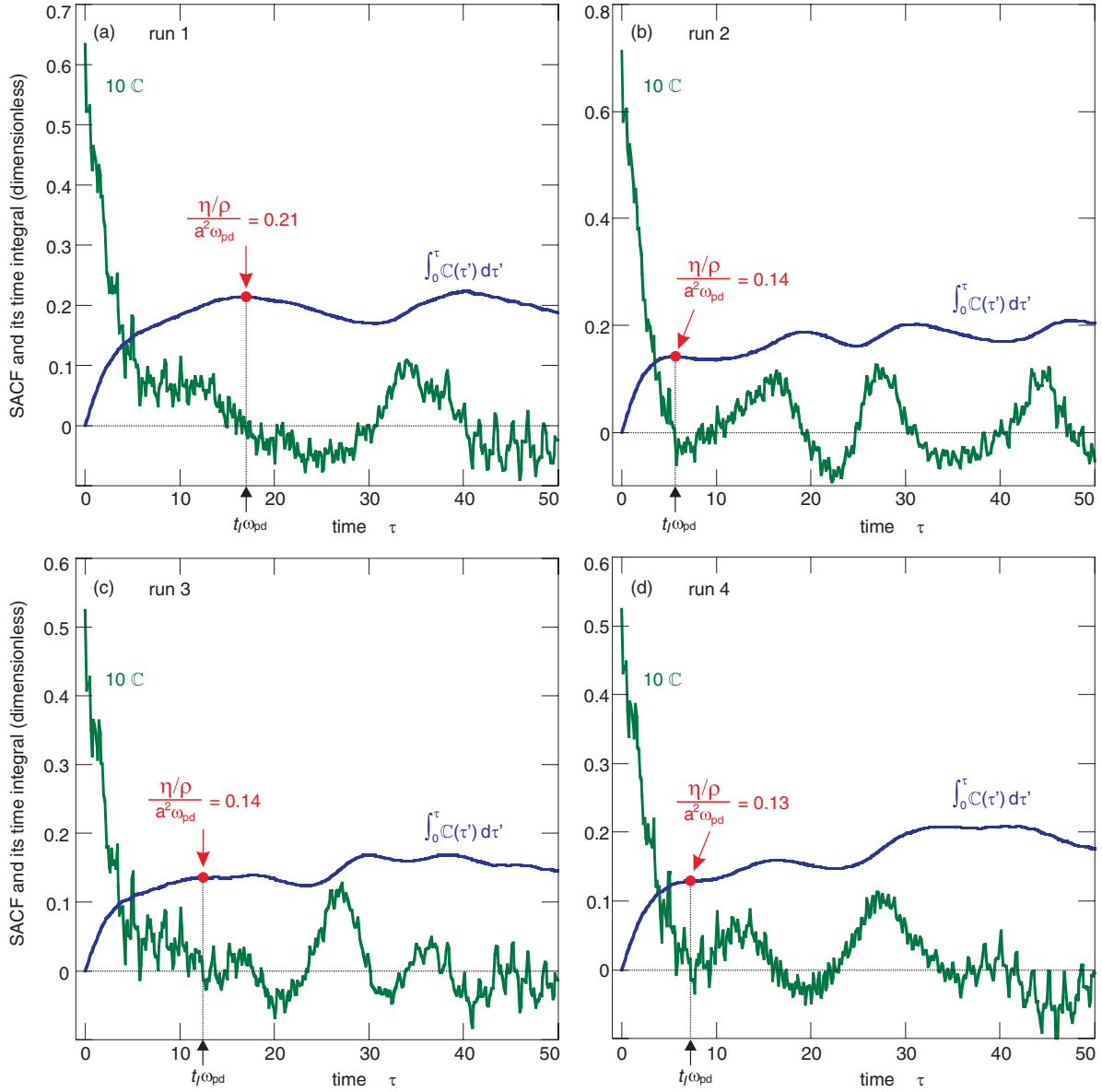


FIG. 3. (Color online) Stress autocorrelation function (SACF), i.e., $C_\eta(t)$, and its time integration. Results are shown for four runs of the experiment [8]. All quantities shown are normalized. The SACF is normalized as $\mathbb{C} \equiv C_\eta / (Ak_B T \rho a^2 \omega_{pd}^2)$ and is drawn here at $10\times$ magnification. Time is given in units of ω_{pd}^{-1} , that is, $\tau = t\omega_{pd}$. The integral shown by the smooth curve is used in the Green-Kubo relation, Eq. (7), to calculate the viscosity. Choosing the integration limit t_l as the time when $\mathbb{C}(\tau)$ crosses zero as described in Sec. IV D, the integral yields the dimensionless viscosity, as indicated by the solid circle for each run.

VI. RESULT FOR VISCOSITY USING THE GREEN-KUBO RELATION WITH EXPERIMENTAL DATA

We now present our result for the viscosity η using the Green-Kubo relation, Eqs. (5)–(7). We report the kinematic viscosity, η/ρ , to enable a convenient comparison to other experiments and simulations.

We find $\eta/\rho = 0.16 \pm 0.02$ in units of $a^2\omega_{pd}$. The value of the normalization factor for the experiment [8] is $a^2\omega_{pd} = 3.7 \times 10^{-6} \text{ m}^2/\text{s}$, while the areal mass density is $\rho = 1.1 \times 10^{-6} \text{ kg}/\text{m}^2$. The value of 0.16 is the mean of the four experimental runs in the presence of laser heating, as plotted in Fig. 3. The error estimate of ± 0.02 , calculated as the standard deviation of the mean, indicates the run-to-run random variation.

VII. DISCUSSION

A. Test of the Green-Kubo relation

Our most significant result is a test of the Green-Kubo relation for viscosity, using as an input experimental data. We perform this test by comparing our result $\eta/\rho = 0.16 \pm 0.02$ to the previously reported result, from a dusty plasma experiment [31] that used a hydrodynamical approach.

In this experiment of Nosenko and Goree, the dust particles flowed in their quasi-2D layer with a macroscopic velocity gradient, allowing a determination of viscosity using a Navier-Stokes equation of motion for the local flow velocity of the dust particles. In contrast with [31], in our analysis here we

TABLE I. Results for the kinematic viscosity η/ρ , which is normalized here by $a^2\omega_{pd}$ to make it dimensionless. Viscosity η is reported as the mean for multiple runs; the standard deviation σ and standard deviation of the mean σ_M are listed.

| Data source | Calculation procedure | Data size | | | | η/ρ , units ($a^2\omega_{pd}$) | | |
|------------------------------|-----------------------|---------------|----------------|--|------|--|-------------|-------------|
| | | M | N | run duration | runs | mean | σ | σ_M |
| experiment [8] | Eq. (5)→(6)→(7) | ≈ 600 | ≈ 2100 | $\approx 607\omega_{pd}^{-1}$ (20.2 s) | 4 | 0.16 | 0.04 | 0.02 |
| Langevin simulation (Sec. V) | Eq. (5)→(6)→(7) | 600 | 4096 | $607\omega_{pd}^{-1}$ | 48 | 0.24 | 0.08 | 0.01 |
| equilibrium simulation [24] | Eq. (1)→(6)→(7) | 4096 | 4096 | $1.86 \times 10^4 \omega_{pd}^{-1}$ | 4 | 0.26 | 0.02 | 0.01 |
| Langevin simulation [24] | Eq. (1)→(6)→(7) | 4096 | 4096 | $1.86 \times 10^4 \omega_{pd}^{-1}$ | 4 | 0.27 | 0.02 | 0.01 |

consider the dust particles only as individual particles, while in [31] data for individual particles were averaged to allow considering the dust particles as a continuum, as is necessary for a hydrodynamical approach. Both experiments, [8] and [31], were performed in the same chamber, and both had a quasi-2D layer of dust particles. The reported values of κ were nearly the same, $\kappa = 0.53$ for [31] and 0.5 for [8]. The electrical interactions among dust particles were much stronger than gas friction, $\omega_{pd} \gg \nu_f$, in both experiments. A difference in the experimental conditions was that the two laser beams were manipulated differently so that in [31] they produced a macroscopic velocity gradient, while in [8] there was heating without a macroscopic velocity gradient.

Considering the complexity of the dusty plasma and our simplifications in describing it, we cannot expect our result to agree with the results of [31] better than within about a factor of 2. In fact, we find agreement within the error bars when comparing our result $\eta/\rho = 0.16 \pm 0.02$ using the Green-Kubo relation and the range of values reported by Nosenko and Goree in [31], Fig. 4.

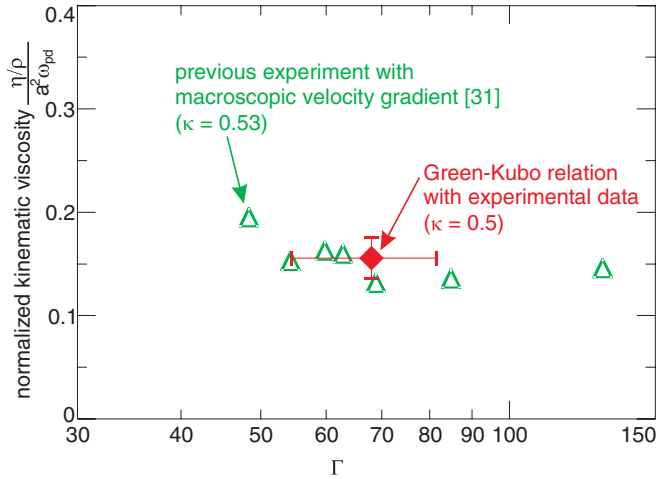


FIG. 4. (Color online) Test of the Green-Kubo relation for viscosity. We compare our value of the kinematic viscosity, calculated from the Green-Kubo relation, using input from the experiment [8], to results from a hydrodynamical analysis of a previous experiment [31]. Values are made dimensionless by normalizing by $a^2\omega_{pd}$. The x axis, which has a logarithmic scale, is the Coulomb coupling parameter Γ as defined in Sec. III. Our result, shown as a solid diamond, is the mean for four experimental runs in Fig. 3, and the vertical error bar indicates only the run-to-run variation, calculated as the standard deviation of the mean. The horizontal error bar (for the result from the Green-Kubo relation) reflects a 10% uncertainty in Q .

B. Comparison to simulations

We also compare our result from the Green-Kubo relation to the available data for viscosity from the simulation literature, Fig. 5. All these data are from 2D MD simulations with a Debye-Hückel potential, and most of them use the Green-Kubo relation, except for the nonequilibrium simulation of [35], which used a so-called nonequilibrium simulation method to produce a macroscopic velocity gradient. We find that the simulations predicted values that are larger, by about a factor of 2, than our result for the Green-Kubo relation using experimental input.

The discrepancy between our result here and the simulation results in Fig. 5 could arise from the differences between the simulations and the experiment [8]. These differences include the use of periodic boundary conditions in the simulations to mimic an infinite system, while the dust particles in the experiment fill a finite region due to dc radial electric fields.

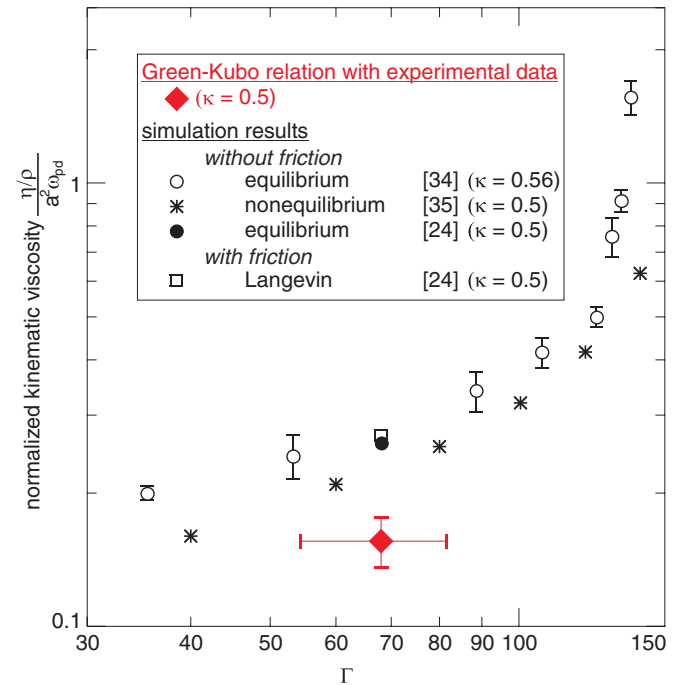


FIG. 5. (Color online) Comparison of our result using the Green-Kubo relation for viscosity with the input of data from the experiment [8], shown as a diamond as in Fig. 4, to values from previously reported 2D Debye-Hückel simulations [24,34,35]. The simulation results shown for [24] are also listed in Table I. Both axes are logarithmic.

While all particles in the simulations are identical, those in the experiment vary in diameter by a few percent [65], with a similar variation in charge. Nonuniformities occur in the simulations only as transients due to fluctuations, while the experiment has static nonuniformities due to the dc radial electric fields. These dc fields induce static stresses that can lead to more structural disorder, which can result in an easier deformation of the arrangement of dust particles and a reduction in the stress required to generate shear flow, which is equivalent to a reduction of the viscosity.

Another possible explanation for the discrepancy with the simulation results is that the potential in the experiment [8] may not be a Debye-Hückel potential, as assumed in Sec. IV A. One alternative, instead of assuming a particular form for the potential, could be an empirically determined potential of mean force, calculated from an experimentally measured pair correlation function, as has been proposed theoretically [15,66]. An advantage of this approach is that all physical processes that affect the potential would be included in the empirical result [66].

VIII. CONCLUSIONS

The Green-Kubo relation for viscosity has been tested using an input of experimental data. The value for the viscosity determined by the Green-Kubo relation with the input of data

from an experiment [8] was compared to the value from a previous experiment using a hydrodynamical method [31]. In both experiments, the physical system was a quasi-2D dusty plasma, and the conditions were similar, aside from the absence of a macroscopic velocity gradient in the experiment [8] for the Green-Kubo result. We found that the results agree as well as can be expected. This agreement serves as a test of the Green-Kubo relation for viscosity of a dusty plasma.

Additionally, we compared our result for the viscosity determined by the Green-Kubo relation with the predictions of MD simulations [24,34,35]. The results were as consistent as expected, given the differences between the simulations and the experiment [8] that provided our input data.

Further tests are needed for other Green-Kubo relations. Because the Green-Kubo relations for the various transport coefficients are all different, a test of the Green-Kubo relation for viscosity, as we have presented here, does not also serve as a test of another Green-Kubo relation. In addition, tests for other physical systems, such as the 2D systems mentioned in Sec. I, would be useful.

ACKNOWLEDGMENTS

This work was supported by the NSF and NASA.

-
- [1] C. A. Murray, W. O. Sprenger, and R. A. Wenk, *Phys. Rev. B* **42**, 688 (1990).
- [2] P. M. Reis, R. A. Ingale, and M. D. Shattuck, *Phys. Rev. Lett.* **96**, 258001 (2006).
- [3] C. C. Grimes and G. Adams, *Phys. Rev. Lett.* **42**, 795 (1979).
- [4] T. B. Mitchell, J. J. Bollinger, X.-P. Huang, W. M. Itano, and D. H. E. Dubin, *Phys. Plasmas* **6**, 1751 (1999).
- [5] P. K. Shukla and A. A. Mamun, *Introduction to Dusty Plasma Physics* (Institute of Physics, Bristol, 2002).
- [6] G. E. Morfill and A. V. Ivlev, *Rev. Mod. Phys.* **81**, 1353 (2009).
- [7] A. Piel, *Plasma Physics* (Springer, Heidelberg, 2010).
- [8] Y. Feng, J. Goree, and B. Liu, *Phys. Rev. Lett.* **105**, 025002 (2010).
- [9] G. K. Batchelor, *An Introduction to Fluid Dynamics* (Cambridge University Press, Cambridge, 1967).
- [10] M. S. Murillo, *Phys. Rev. Lett.* **85**, 2514 (2000).
- [11] G. Salin, *Phys. Plasmas* **14**, 082316 (2007).
- [12] P. K. Kaw and A. Sen, *Phys. Plasmas* **5**, 3552 (1998).
- [13] M. S. Green, *J. Chem. Phys.* **20**, 1281 (1952); **22**, 398 (1954).
- [14] R. Kubo, *J. Phys. Soc. Jpn.* **12**, 570 (1957).
- [15] J. P. Hansen and I. R. McDonald, *The Theory of Simple Liquids*, 2nd ed. (Elsevier Academic, Amsterdam, 1986).
- [16] Z. Donkó, P. Hartmann, and J. Goree, *Mod. Phys. Lett. B* **21**, 1357 (2007).
- [17] R. Pal, *J. Colloid Interface Sci.* **225**, 359 (2000).
- [18] T. G. Mason and D. A. Weitz, *Phys. Rev. Lett.* **74**, 1250 (1995).
- [19] J. C. Crocker, M. T. Valentine, E. R. Weeks, T. Gisler, P. D. Kaplan, A. G. Yodh, and D. A. Weitz, *Phys. Rev. Lett.* **85**, 888 (2000).
- [20] B. J. Alder and T. E. Wainwright, *Phys. Rev. Lett.* **18**, 988 (1967); *Phys. Rev. A* **1**, 18 (1970).
- [21] M. H. Ernst, E. H. Hauge, and J. M. J. van Leeuwen, *Phys. Rev. Lett.* **25**, 1254 (1970); J. R. Dorfman and E. G. D. Cohen, *ibid.* **25**, 1257 (1970).
- [22] C. K. Goertz, *Rev. Geophys.* **27**, 271 (1989).
- [23] D. Samsonov, J. Goree, H. M. Thomas, and G. E. Morfill, *Phys. Rev. E* **61**, 5557 (2000).
- [24] Y. Feng, J. Goree, and B. Liu, *Phys. Plasmas* **18**, 057301 (2011).
- [25] X. Wang, A. Bhattacharjee, and S. Hu, *Phys. Rev. Lett.* **86**, 2569 (2001).
- [26] G. Joyce, M. Lampe, and G. Ganguli, *IEEE Trans. Plasma Sci.* **29**, 238 (2001).
- [27] L. Bonsall and A. A. Maradudin, *Phys. Rev. B* **15**, 1959 (1977).
- [28] V. Nosenko, J. Goree, and A. Piel, *Phys. Plasmas* **13**, 032106 (2006).
- [29] The different roles of the dust particles and the neutral gas in determining the transfer of momentum can be illustrated by comparing a dusty plasma to a dilute colloidal suspension. The latter consists of two components: solid particles and a liquid solvent such as water, which have comparable mass densities. If the solid particles are sufficiently small, they are dragged along in the flow of the solvent, so that the local velocities of the solid particles and solvent are nearly the same (G. K. Batchelor, Ref. [9]). Then, the two components of a dilute colloidal suspension can be considered to be moving as one, which has an effective viscosity that is slightly larger than that of the pure solvent according to Einstein's result [A. Einstein, *Ann. Phys.* **339**, 591 (1911)]. A dusty plasma is different because instead

of a liquid solvent, there is a rarefied gas, which is many orders of magnitude less dense. Then the dust particles can flow with a velocity that is different from that of the rarefied gas as a whole. This difference in velocity between a dust particle and the gas as a whole leads to a friction between them, which is different from the viscous friction due to collisions among the dust particles via their electrical repulsion.

- [30] W.-T. Juan, M.-H. Chen, and L. I, *Phys. Rev. E* **64**, 016402 (2001).
- [31] V. Nosenko and J. Goree, *Phys. Rev. Lett.* **93**, 155004 (2004).
- [32] A. Gavrikov, I. Shakhova, A. Ivanov, O. Petrov, N. Vorona, and V. Fortov, *Phys. Lett. A* **336**, 378 (2005).
- [33] N. A. Vorona, A. V. Gavrikov, A. S. Ivanov, O. F. Petrov, V. E. Fortov, and I. A. Shakhova, *J. Exp. Theor. Phys.* **105**, 824 (2007).
- [34] B. Liu and J. Goree, *Phys. Rev. Lett.* **94**, 185002 (2005).
- [35] Z. Donkó, J. Goree, P. Hartmann, and K. Kutasi, *Phys. Rev. Lett.* **96**, 145003 (2006).
- [36] Z. Donkó, J. Goree, P. Hartmann, and B. Liu, *Phys. Rev. E* **79**, 026401 (2009).
- [37] D. A. McQuarrie, *Statistical Mechanics* (Harper & Row, New York, 1976).
- [38] O. S. Vaulina, X. G. Adamovich, O. F. Petrov, and V. E. Fortov, *Phys. Rev. E* **77**, 066404 (2008).
- [39] O. S. Vaulina, K. G. Adamovich, O. F. Petrov, and V. E. Fortov, *J. Exp. Theor. Phys.* **107**, 313 (2008).
- [40] R. A. L. Jones, *Soft Condensed Matter* (Oxford University Press, Auckland, 2003).
- [41] B. Liu, J. Goree, and O. S. Vaulina, *Phys. Rev. Lett.* **96**, 015005 (2006).
- [42] G. J. Kalman, P. Hartmann, Z. Donkó, and M. Rosenberg, *Phys. Rev. Lett.* **92**, 065001 (2004).
- [43] S. Ichimaru, *Rev. Mod. Phys.* **54**, 1017 (1982).
- [44] Y. Feng, J. Goree, and B. Liu, *Rev. Sci. Instrum.* **78**, 053704 (2007).
- [45] Y. Feng, J. Goree, and B. Liu, *Rev. Sci. Instrum.* **82**, 053707 (2011).
- [46] M. Wolter and A. Melzer, *Phys. Rev. E* **71**, 036414 (2005).
- [47] A. Melzer, S. Nunomura, D. Samsonov, Z. W. Ma, and J. Goree, *Phys. Rev. E* **62**, 4162 (2000).
- [48] B. Liu and J. Goree, *Phys. Rev. Lett.* **100**, 055003 (2008).
- [49] Y. Feng, J. Goree, and B. Liu, *Phys. Rev. Lett.* **100**, 205007 (2008).
- [50] U. Konopka, G. E. Morfill, and L. Ratke, *Phys. Rev. Lett.* **84**, 891 (2000).
- [51] O. S. Vaulina, E. A. Lisin, A. V. Gavrikov, O. F. Petrov, and V. E. Fortov, *J. Exp. Theor. Phys.* **110**, 662 (2010).
- [52] Nonisotropic models have been developed to take into account the effects of ion wakes, which arise from a flow of ions that is driven by the same vertical electric field that levitates the dust particles. Examples include V. A. Schweigert, I. V. Schweigert, A. Melzer, A. Homann, and A. Piel, *Phys. Rev. Lett.* **80**, 5345 (1998); M. Lampe, G. Joyce, G. Ganguli, and V. Gavrishchaka, *Phys. Plasmas* **7**, 3851 (2000); R. Kompaneets, U. Konopka, A. V. Ivlev, U. Tsyrovich, and G. Morfill, *ibid.* **14**, 052108 (2007).
- [53] M. S. Murillo, *Phys. Rev. E* **62**, 4115 (2000).
- [54] T. Saigo and S. Hamaguchi, *Phys. Plasmas* **9**, 1210 (2002).
- [55] G. Salin and J.-M. Caillol, *Phys. Plasmas* **10**, 1220 (2003).
- [56] G. Faussurier, *Phys. Rev. E* **69**, 066402 (2004).
- [57] S. Nunomura, J. Goree, S. Hu, X. Wang, A. Bhattacharjee, and K. Avinash, *Phys. Rev. Lett.* **89**, 035001 (2002).
- [58] S. Nunomura, S. Zhdanov, D. Samsonov, and G. Morfill, *Phys. Rev. Lett.* **94**, 045001 (2005).
- [59] We carried out tests that showed that the SACF is more sensitive to an error in Q than in λ_D .
- [60] Z. Donkó, J. Goree, and P. Hartmann, *Phys. Rev. E* **81**, 056404 (2010).
- [61] F. Reif, *Fundamentals of Statistical and Thermal Physics*, Chap. 15 (McGraw Hill, New York, 1965).
- [62] W. F. van Gunsteren and H. J. C. Berendsen, *Mol. Phys.* **45**, 637 (1982).
- [63] T. Ott and M. Bonitz, *Phys. Rev. Lett.* **103**, 195001 (2009).
- [64] For comparison, the memory time of collective motion in this liquid of dust particles was $\approx 10\omega_{pd}^{-1}$, as measured by the zero crossing of the correlation function $C_\eta(t)$.
- [65] B. Liu, J. Goree, V. Nosenko, and L. Boufendi, *Phys. Plasmas* **10**, 9 (2003).
- [66] U. de Angelis, *Phys. Plasmas* **8**, 1751 (2001).